Supporting Information

for

Straightforward and selective metal capture through CO_2-induced self-assembling

Guillaume Poisson,[ab] G. Germain,[a] J. Septavaux,[a] Julien Leclaire,*[ab]

Content

1. General methods

1.1. Solvents

All solvents were purified by standard procedures or obtained from a Solvent Purification System (Braun SPS 800).

1.2. Synthesis

1.2.1. Metal salts

4-Fluorophenol (99%), $Ba(OH)_2$ (95%), $BaCl_2$ (99%), CH_3OH (99,6%), Cs_2CO_3 (99%), $Cu(CH_3CO_2)_2.H_2O$ (98%), D_2SO_4 (99,5%), Diethylenetriamine (99%), $FeCl_3.6H_2O$ (98%), In_2O_3 (99%), $MgCl_2$ (99%), Na_2CO_3 (99%), Nd_2O_3 (99,9%), $SrCl_2.6H_2O$ (99%), ZnO (99%) were purchased from Sigma-Aldrich. $Mg(CH_3CO_2).4H_2O$ (99%), $Ni(CH_3CO_2).4H_2O$ (98%), $PdCl_2$ (99,9%), were obtained from Strem Chemicals. EtOH (99,98%) was purchased from VWR. $CoCl_2$ (97%) was purchased from Acros. CO_2 (99,95%) was obtained from Air Liquid. Dy_2O_3 (99,9%), Eu_2O_3 (99,9%), $K(CF_3CO_2)$ (98%), $Li(CF_3CO_2)$ (97%), $Pd(CF_3CO_2)_2$ (97%), $Pr_2(CO_3)_3$ (99,9%), Sm_2O_3 (99,9%), $Tb_2(CO_3)_3$ (99,9%) were purchased from Alfa Aesar. CD_3OD (99,8%) and D_2O (99,9%) were purchased from Eurisotop. $Ca(OH)_2$ (96%) and $CuCl_2.2H_2O$ (99%) was obtained from Merck. $CaCl_2$ (94%) was purchased from Prolabo. K_2CO_3 (99%) was purchased from Riedel-de Haen.

Otherwise stated, trifluoroacetate salts were obtained following the procedure described for lanthanide trifluoroacetate synthesis [1]. $Pr(CF_3CO_2)_3$, $Nd(CF_3CO_2)_3$, $Sm(CF_3CO_2)_3$, $Eu(CF_3CO_2)_3$, $Tb(CF_3CO_2)_3$, $Dy(CF_3CO_2)_3$, $Y(CF_3CO_2)_3$, $Zn(CF_3CO_2)_2$ were obtained from metal oxide. $Ca(CF_3CO_2)_2$, $Ba(CF_3CO_2)_3$, $In(CF_3CO_2)_3$ were synthesized from metal hydroxide. $Na(CF_3CO_2)$ was obtained from sodium carbonate. $In(OH)_3$ was synthesized using the following procedure. An excess of an aqueous solution of nitric acid 68%wt (20mL) was added to a suspension of In_2O_3 (1g, 3,6 mmol) in 5 mL of water. The mixture was refluxed until complete dissolution. Water and remaining acid were removed under reduced pressure. The resulting yellow oil was then dissolved in 5 mL of water and an excess of an aqueous solution 0.5M of KOH was added. Spontaneous precipitation of $In(OH)_3$ occurred. The solid was filtered and wash 4 times with 20mL of water and dried at 70°C under reduced pressure. $In(OH)_3$ can be used for the preparation of $In(CF_3CO_2)_3$ following the procedure reported for lanthanides. $Fe(CF_3CO_2)_3$ was synthesized using procedure described by Iranpoor *et al.* [2].$Co(CF_3CO_2)_2$ salt was obtained using the procedure described by Shap *et al.* [3].

1.2.2. CO_2-based organometallic materials

A 0.5 M solution of diethylenetriamine (540µL; 5,0 mmol) in MeOH (10mL) is added to a trifluoroacetate metal salt (0.416 mmol; 201.4 mg of $Nd(O_2C_2F_3)_3$; 200.0 mg of $Pr(O_2C_2F_3)_3$; 204.6 mg of $Eu(O_2C_2F_3)_3$; 207.5 mg of $Tb(O_2C_2F_3)_3$; 203.9 mg of $Sm(O_2C_2F_3)_3$; 209.0 mg of $Dy(O_2C_2F_3)_3$; 82.3 mf of $Fe(O_2C_2F_3)_3$ (0.21 mmol) and 100.5 mg of $Nd(O_2C_2F_3)_3$ (0.21 mmol); 59.4 mg of $Co(O_2C_2F_3)_2$ (0.21 mmol) and 102.0 mg of $Sm(O_2C_2F_3)_3$ (0.21 mmol)) in a round-bottom flask. The resulting clear solution is purged with CO2, refluxed for an hour then cooled down to room temperature under CO2 atmosphere overnight. The suspension is then centrifuged and the supernatant removed. The solid washed with 2*10mL of MeOH, centrifuged and dry under vacuum. Supernatants are gathered and solvent evaporated under reduced pressure. Each sample is produced in triplicate before analysis.

1.2.3. Metal release through CO_2-departure

Following a typical capturing step as described previously ($c_0 = 0.5$ M, $x_0 = 1/12$), the solid material collected is re-suspended into 10 mL of MeOH. $(1-E_s(X))*n_0$ moles of TFA and $(1-Es(DETA))*n_0$ moles de DETA are then added and the mixture is refluxed under a gentle flux of nitrogen until a clear solution is obtained.

1.3. Nuclear Magnetic Resonance

For substystems **II**, liquid state NMR spectra were recorded in, methanol-d4, heavy water on spectrometers operating at 500 MHz (BBFO and BBI probes with z gradients) respectively for 1H and 13C. Solvent residual signals were used as internal standard (when necessary, water suppression by presaturation was used). 2s relaxation time allowed proton full relaxation. 13C spectra were recorded using a 30 degrees tilt angle and 2s relaxation time. HSQC experiments were run either in full or reduced spectral window (SW = 3.1-2.1 ppm for ^1H and 50-34 ppm for ^{13}C) to optimize the resolution, following reported procedure [4].

For systems **III**, ^{1}H and ^{19}F NMR spectra were recorded on a Bruker Advance 300 spectrometer, operating at a frequency of 300 MHz. The samples were prepared by dissolving 5-10mg of the solid residue in a 1mL vial with 650µL of a 95/5 (v/v) D_2O/D_2SO4 solution containing 0.06 mol.L^{-1} 4-fluorophenol as an internal standard and sonicated for 3 h at 50°C, then transferred into a NMR tube for 1D standard analysis. 16s relaxation time allowed proton and fluorine full relaxation.

1.4. Volumetric analysis

Analysis were performed with a home-made Chittick Apparatus at 0°C in an ice bath. Calibration was conducted with K_2CO_3 to relate the volume measured to the molar content in carbon dioxide. In a typical experiment, 30mg of solid material were digested by adding under vigorous stirring an excess (1mL) of a 1M H_2SO_4 solution.

1.5. ICP-OES analysis

ICP-OES analysis were recorded on a Varian ICP-OES 710ES. The samples were prepared by dissolving 30 mg of solid or supernatant residue in an aqueous solution of HNO_3 69%wt for standard acid digestion. Each solution was then precisely diluted in order to reach the successive estimated concentrations of 100, 200 and 400 ppb of metal. All samples were analyzed at 3 different wavelengths in triplicate mode.

1.6. UV-Vis analysis

UV-Vis spectra were recorded on a Shimadzu UV-2401 PC spectrophotometer. The samples were prepared by dissolving 15mg of solid residue in an aqueous solution of HCl 5%wt. The solution was then precisely diluted to reach levels of absorbance at the working wavelength were the Beer Lambert law is valid. Nd^{3+} was quantified at $\lambda = 794$ nm, Dy^{3+} was quantified at $\lambda = 806$ nm and Fe^{3+} at $\lambda = 334.5$ nm. As Nd^{3+} also absorbs around 334.5 nm, a cross-calibration was required to reliably determine the concentration in Fe^{3+}.

2. Individual datasets

2.1. NMR of sub-systems II

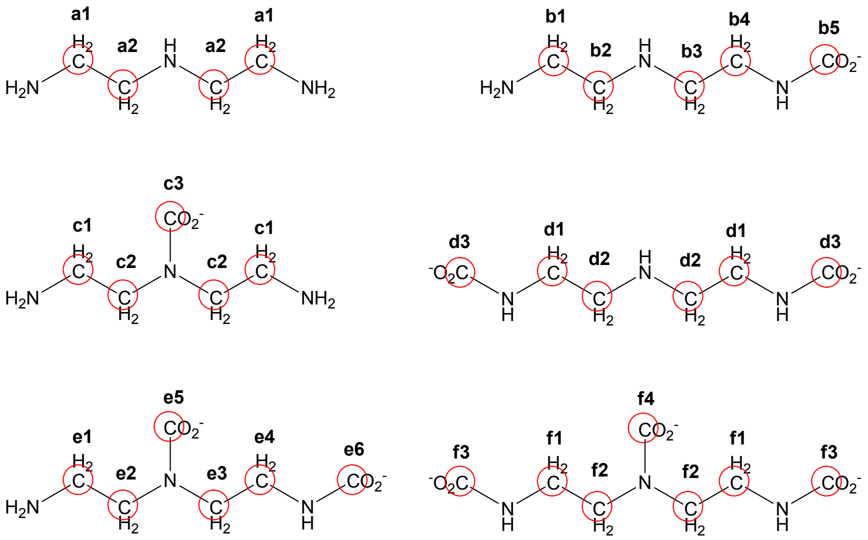

2.1.1. 2.5 M in D_2O

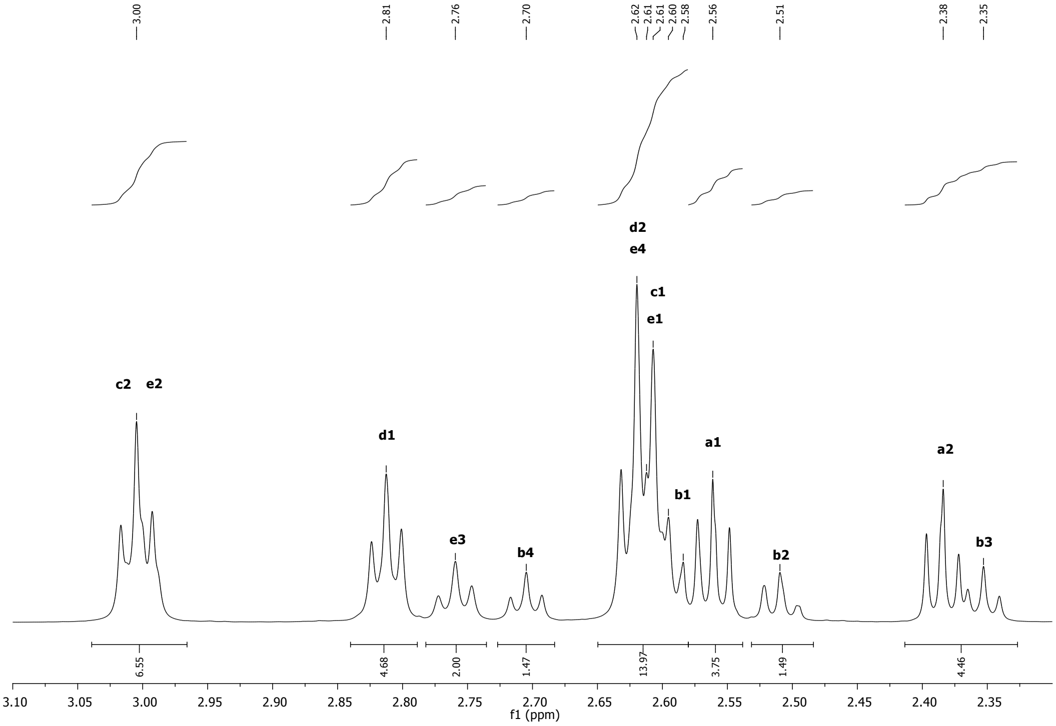

Figure S1: ^{1}H NMR spectrum of a 2.5 M solution of DETA in D_2O purged with CO_2, refluxed for an hour then cooled down to room temperature under CO_2 atmosphere overnight.

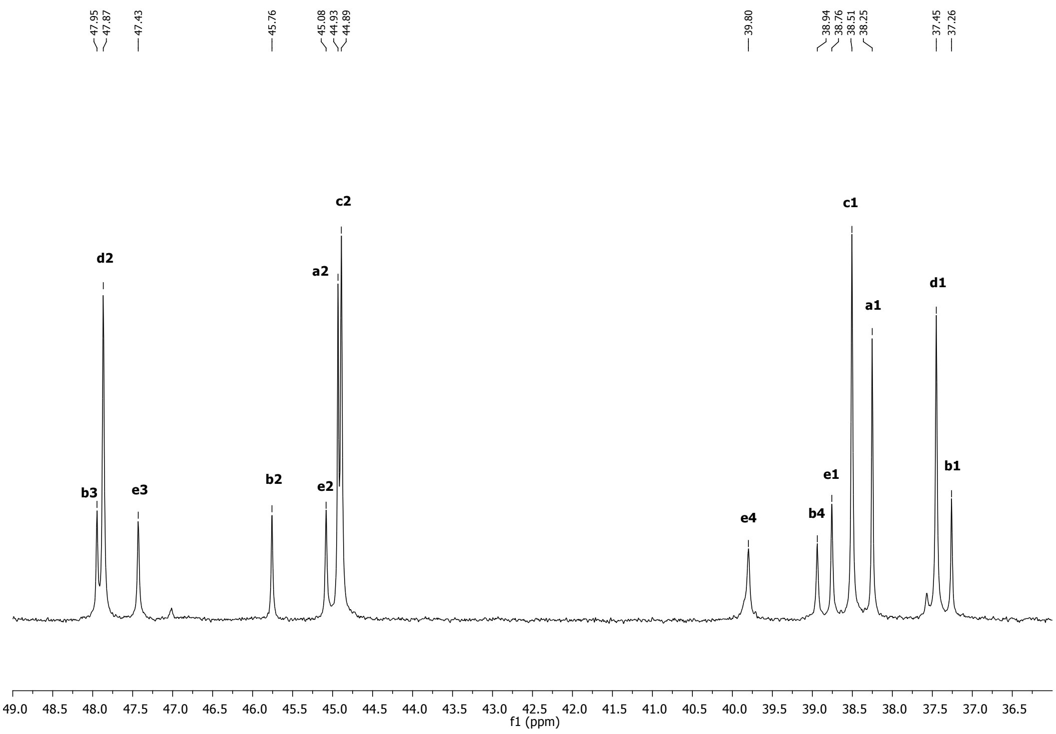

Figure S2: High field ^{13}C NMR spectrum of a 2.5 M solution of DETA in D_2O purged with CO_2, refluxed for an hour then cooled down to room temperature under CO_2 atmosphere overnight.

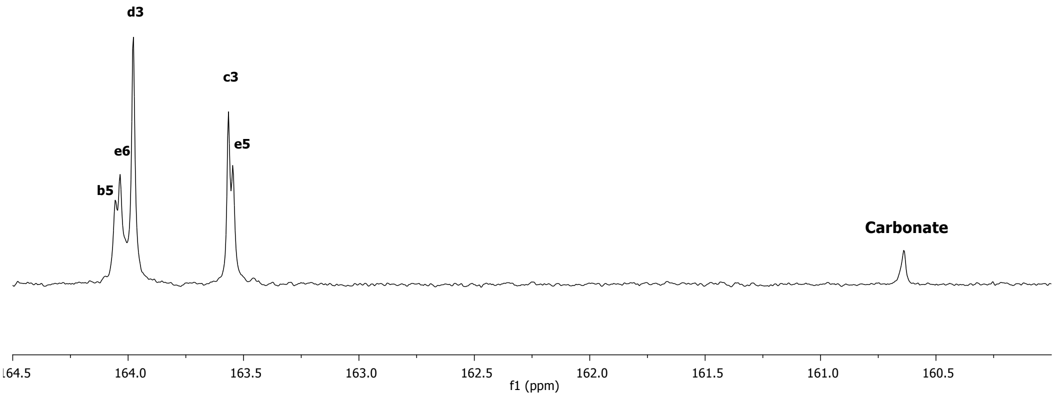

Figure S3: Low field ^{13}C NMR spectrum of a 2.5 M solution of DETA in D_2O purged with CO_2, refluxed for an hour then cooled down to room temperature under CO_2 atmosphere overnight.

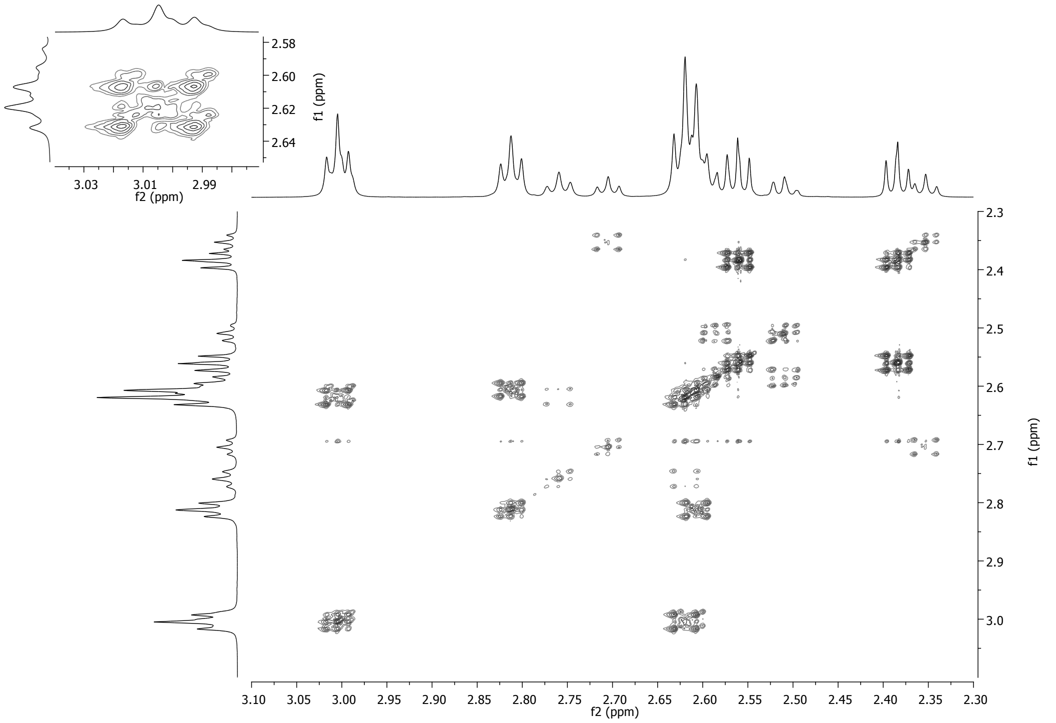

Figure S3: COSY NMR spectrum of a 2.5 M solution of DETA in D_2O purged with CO_2, refluxed for an hour then cooled down to room temperature under CO_2 atmosphere overnight.

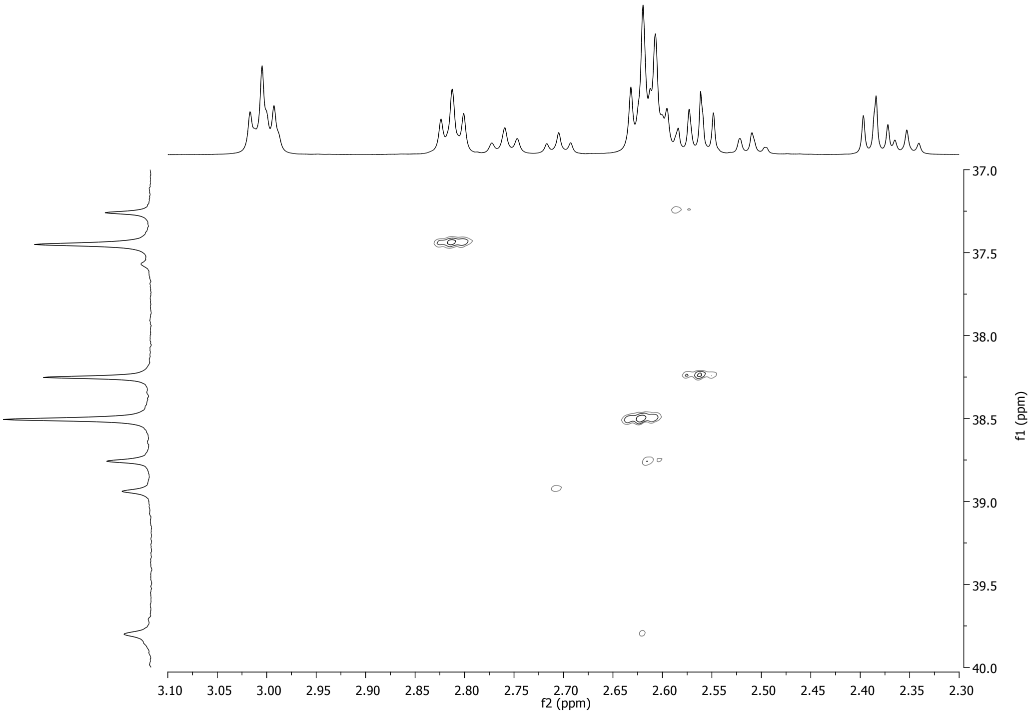

Figure S4: Partial view of the HSQC NMR spectrum of a 2.5 M solution of DETA in D_2O purged with CO_2, refluxed for an hour then cooled down to room temperature under CO_2

atmosphere overnight.

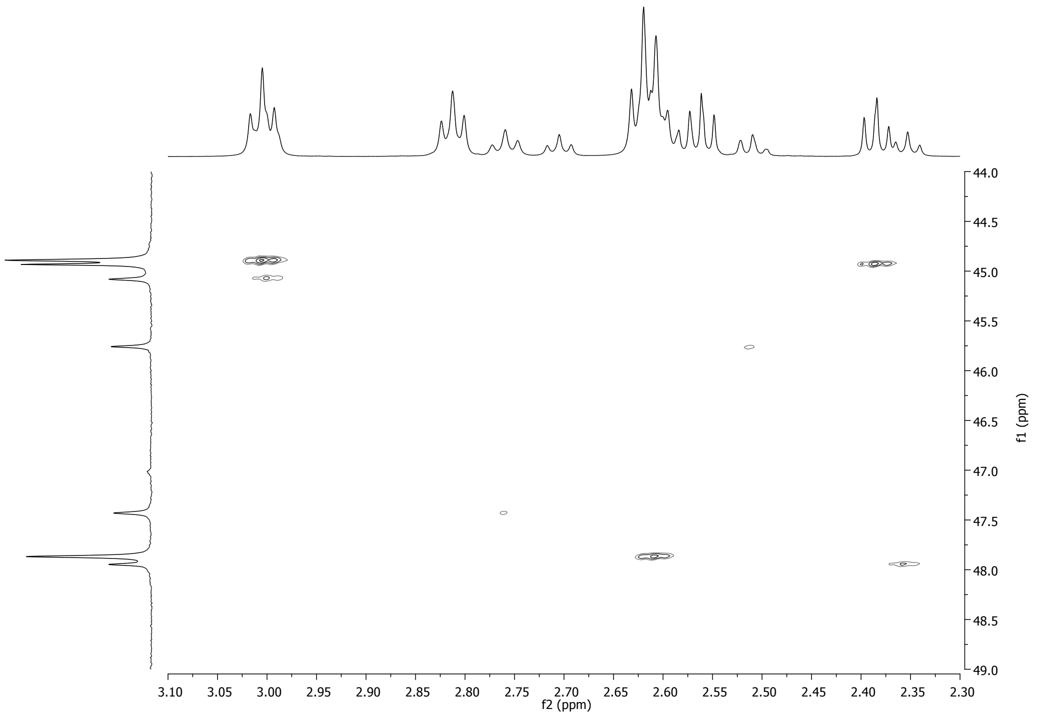

Figure S5: Partial view of the HSQC NMR spectrum of a 2.5 M solution of DETA in D_2O purged with CO_2, refluxed for an hour then cooled down to room temperature under CO_2 atmosphere overnight.

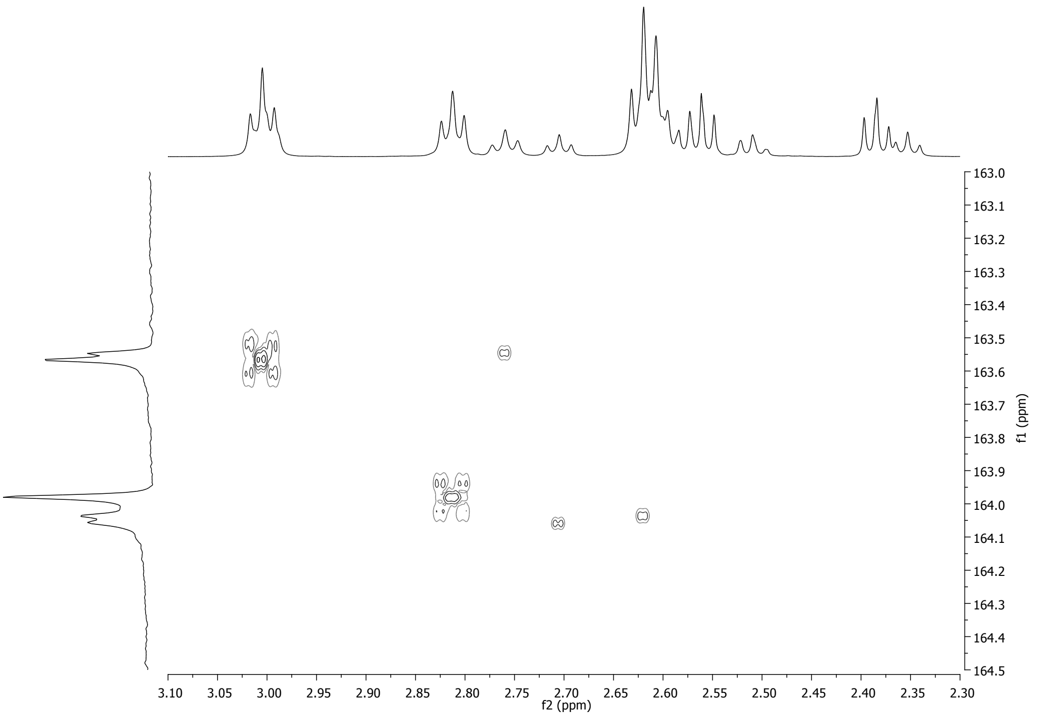

Figure S6: View of the low field HMBC NMR spectrum of a 2.5 M solution of DETA in D_2O purged with CO_2, refluxed for an hour then cooled down to room temperature under CO_2 atmosphere overnight..

2.1.2. 0.5 M in D_2O

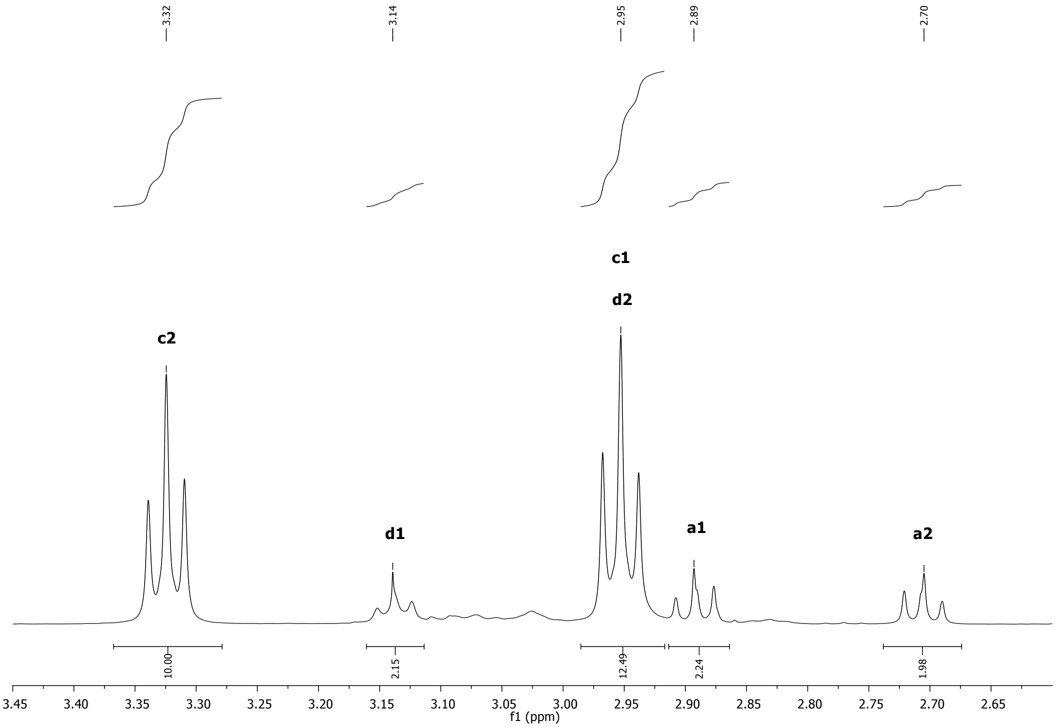

Figure S7: ^1H NMR spectrum of a 0.5 M solution of DETA in D_2O purged with CO_2, refluxed for an hour then cooled down to room temperature under CO_2 atmosphere overnight

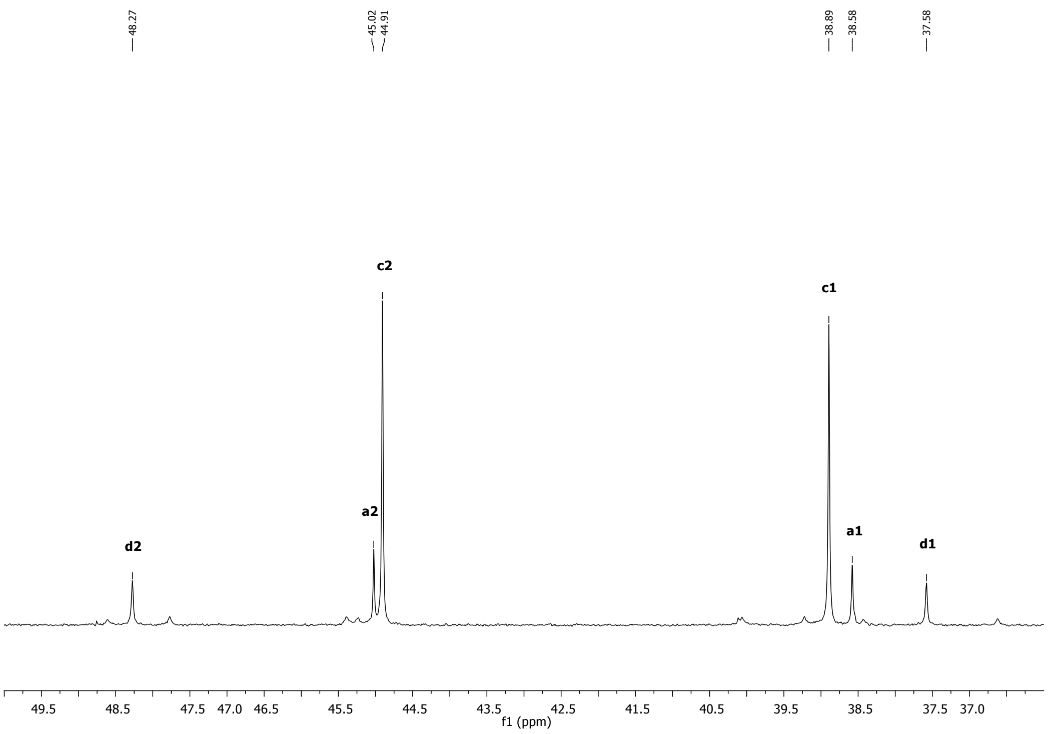

Figure S8: High field ^{13}C NMR spectrum of a 0.5 M solution of DETA in D_2O purged with CO_2, refluxed for an hour then cooled down to room temperature under CO_2 atmosphere overnight.

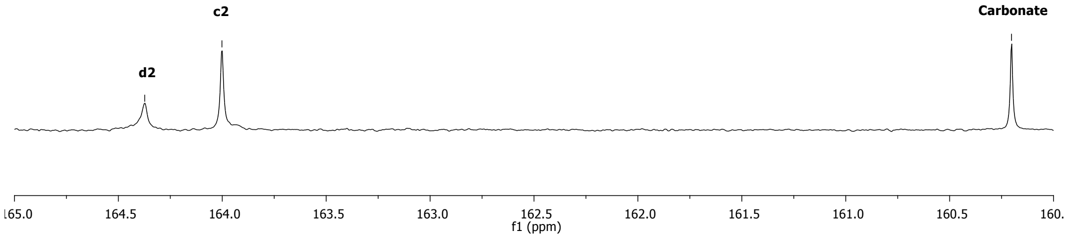

Figure S8: Low field ^{13}C NMR spectrum of a 0.5 M solution of DETA in D_2O purged with CO_2, refluxed for an hour then cooled down to room temperature under CO_2 atmosphere overnight.

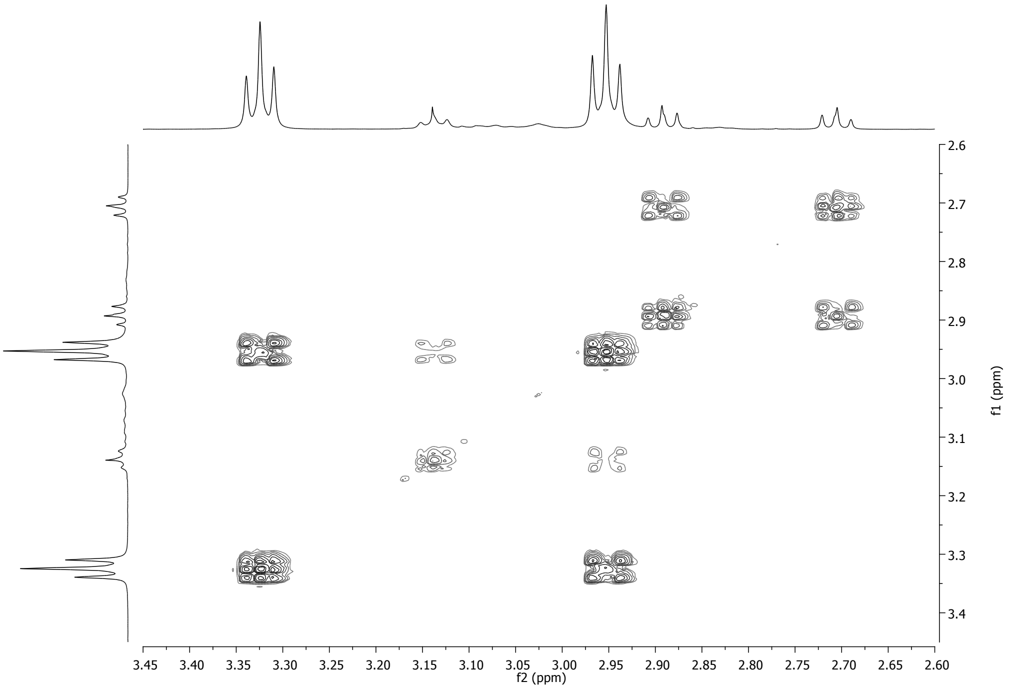

Figure S9: COSY NMR spectrum of a 0.5 M solution of DETA in D_2O purged with CO_2, refluxed for an hour then cooled down to room temperature under CO_2 atmosphere overnight.

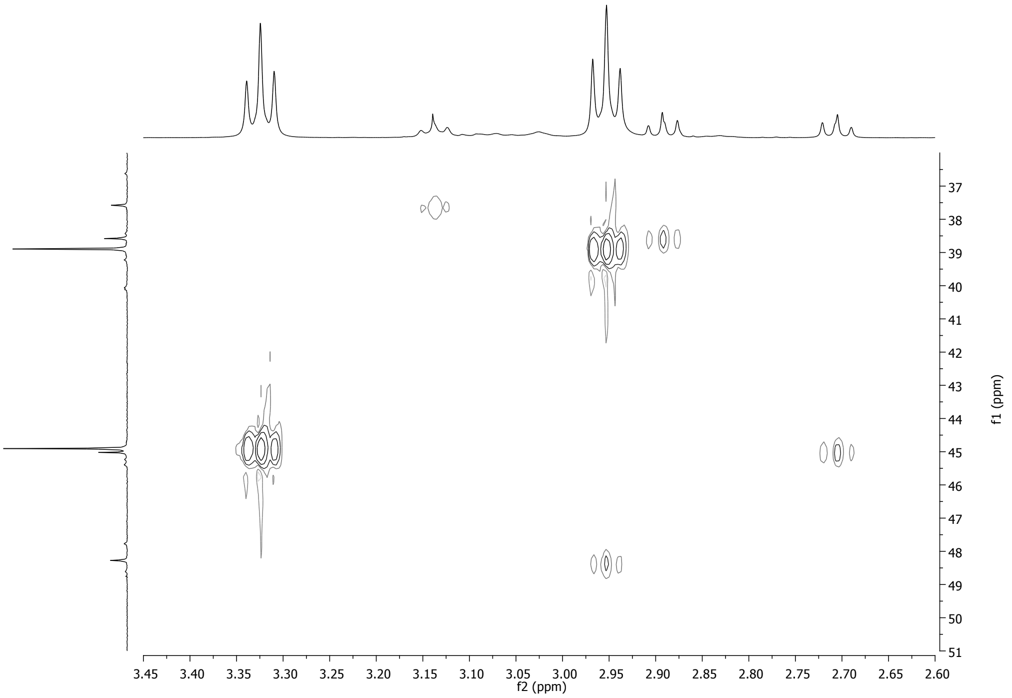

Figure S10: HSQC NMR spectrum of a 0.5 M solution of DETA in D_2O purged with CO_2, refluxed for an hour then cooled down to room temperature under CO_2 atmosphere overnight.

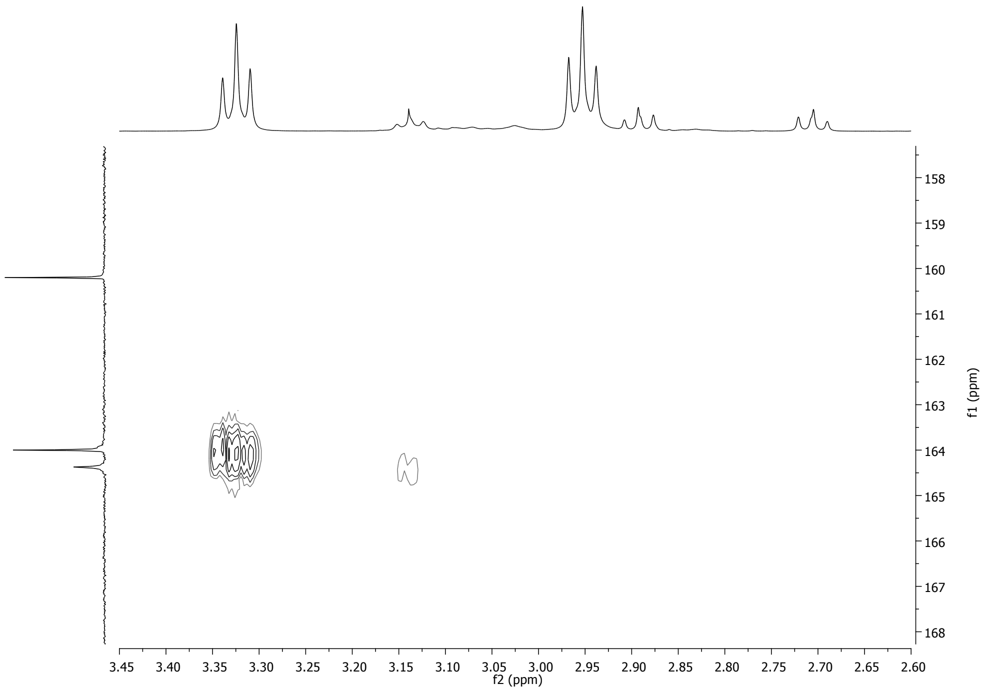

Figure S11: Partial view of the low field HMBC NMR spectrum of a 0.5 M solution of DETA in D_2O purged with CO_2, refluxed for an hour then cooled down to room temperature under CO_2 atmosphere overnight.

2.1.3. 0.5 M in CD$_3$OD

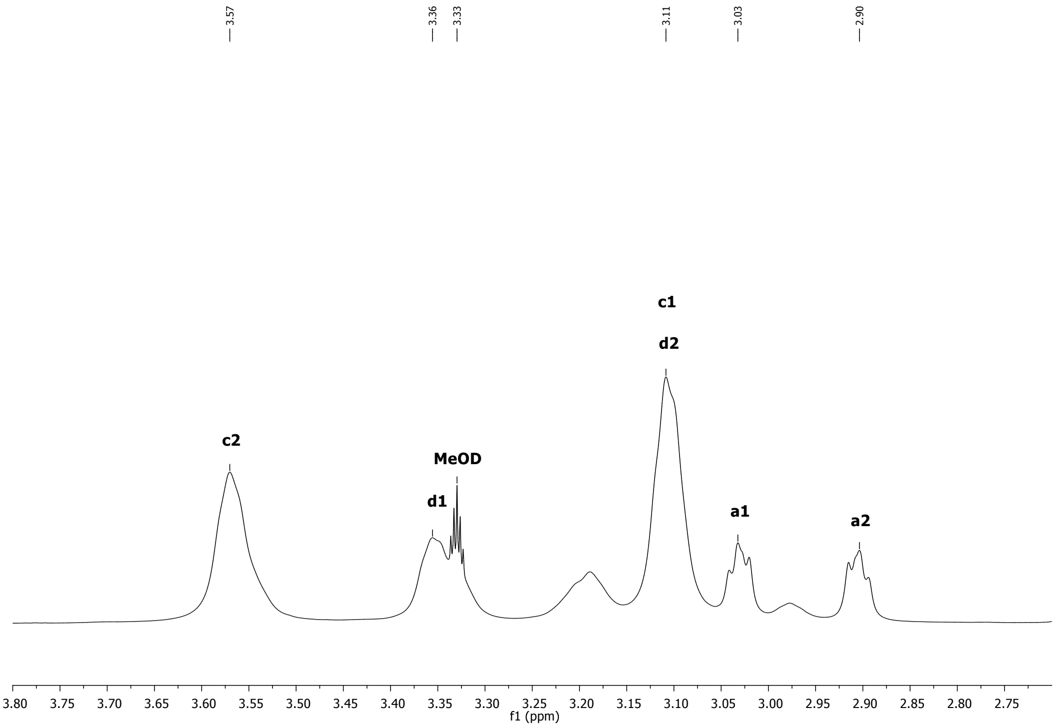

Figure S12: ^{1}H NMR spectrum of a 0.5 M solution of DETA in CD$_3$OD purged with CO$_2$, refluxed for an hour then cooled down to room temperature under CO$_2$ atmosphere overnight..

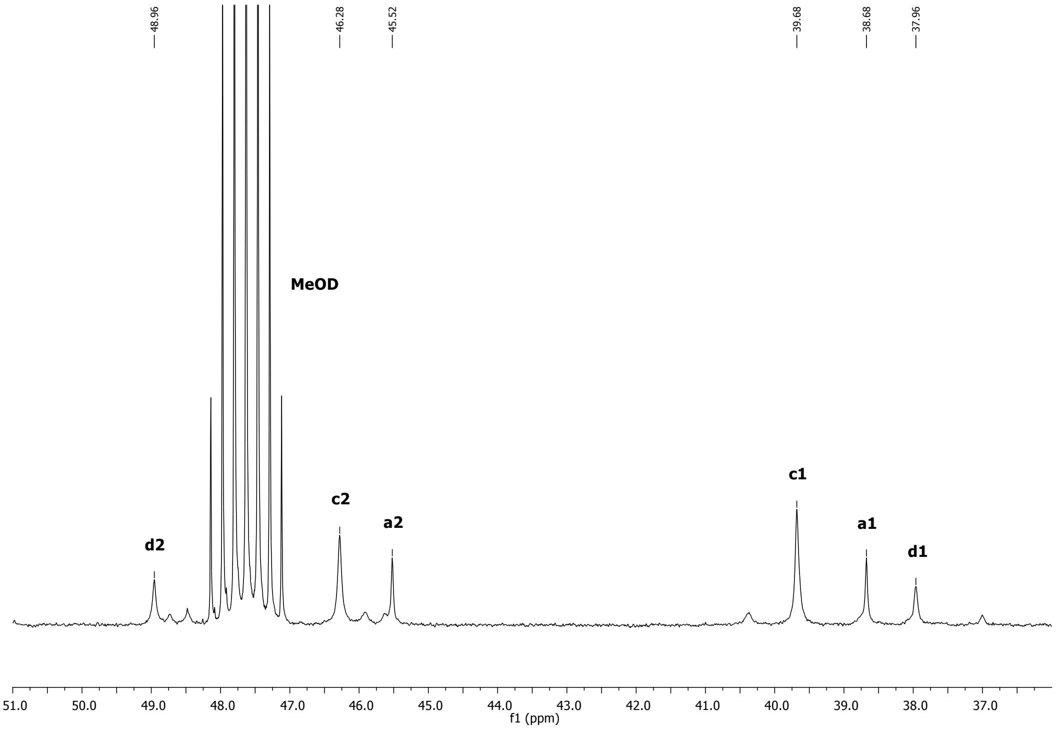

Figure S13: High field of ^{13}C NMR spectrum of a 0.5 M solution of DETA in CD_3OD purged with CO2, refluxed for an hour then cooled down to room temperature under CO_2 atmosphere overnight.

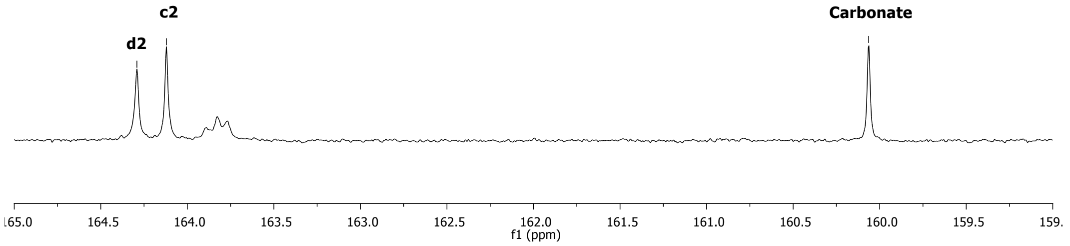

Figure S14: Low field of ^{13}C NMR spectrum of a 0.5 M solution of DETA in CD_3OD purged with CO_2, refluxed for an hour then cooled down to room temperature under CO_2 atmosphere overnight.

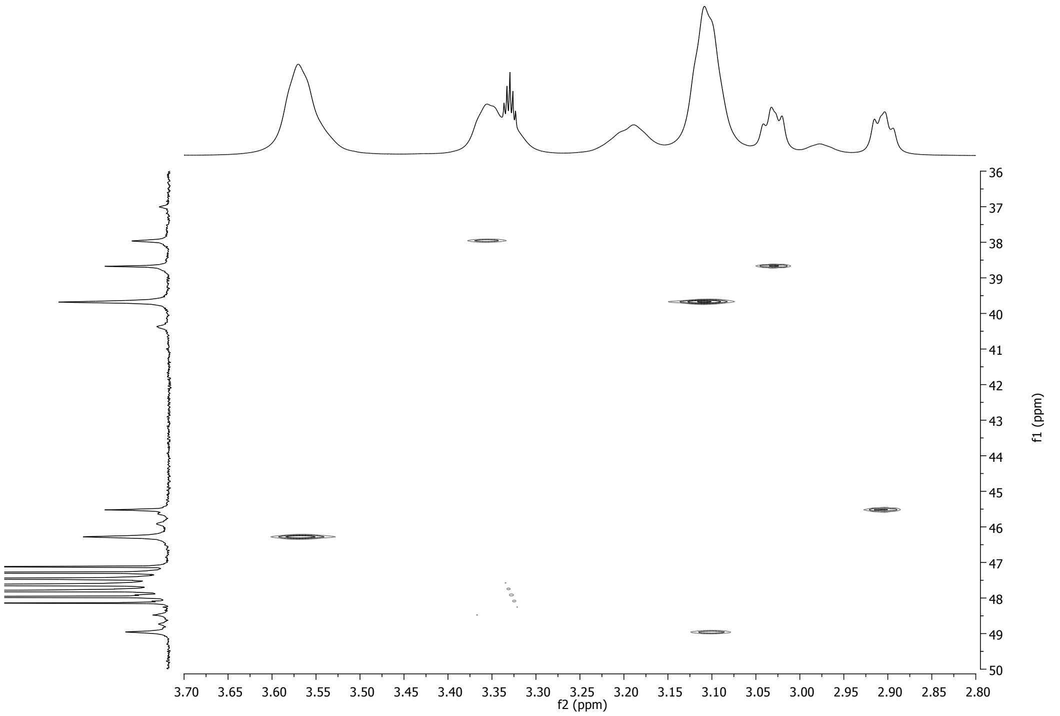

Figure S15: HSQC NMR spectrum of a 0.5 M solution of DETA in CD_3OD purged with CO_2, refluxed for an hour then cooled down to room temperature under CO_2 atmosphere overnight.

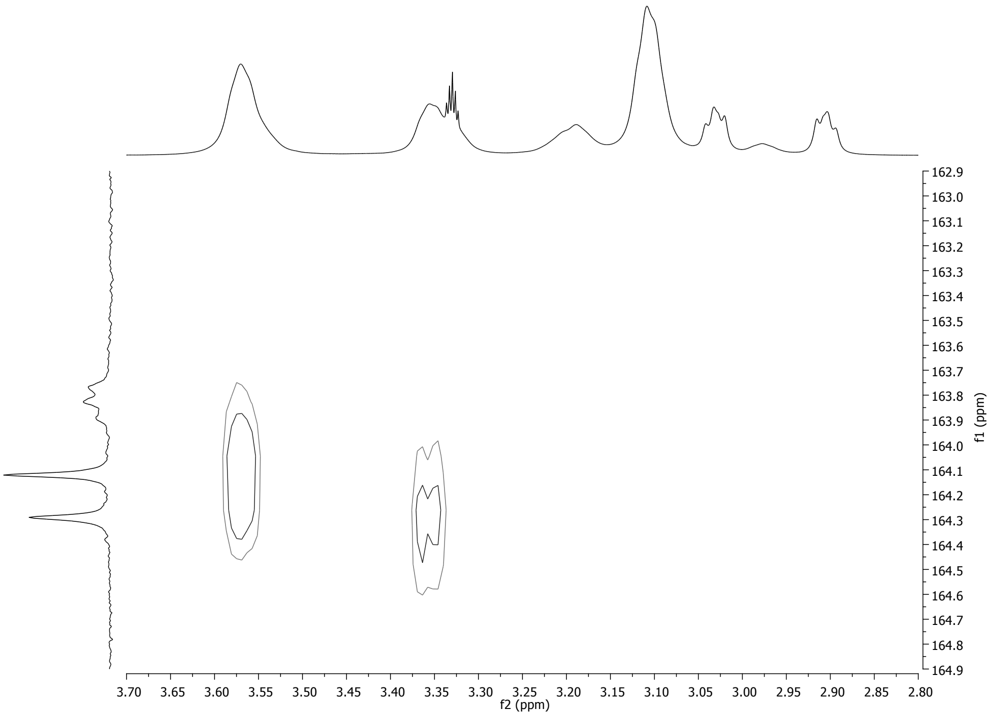

Figure S16: Partial view of the low field HMBC NMR spectrum of a 0.5 M solution of DETA in CD_3OD purged with CO_2, refluxed for an hour then cooled down to room temperature under CO_2 atmosphere overnight.

2.2. Constitutent analyses of systems III

2.2.1. Monometal systems

2.2.1.1. Influence of the metal

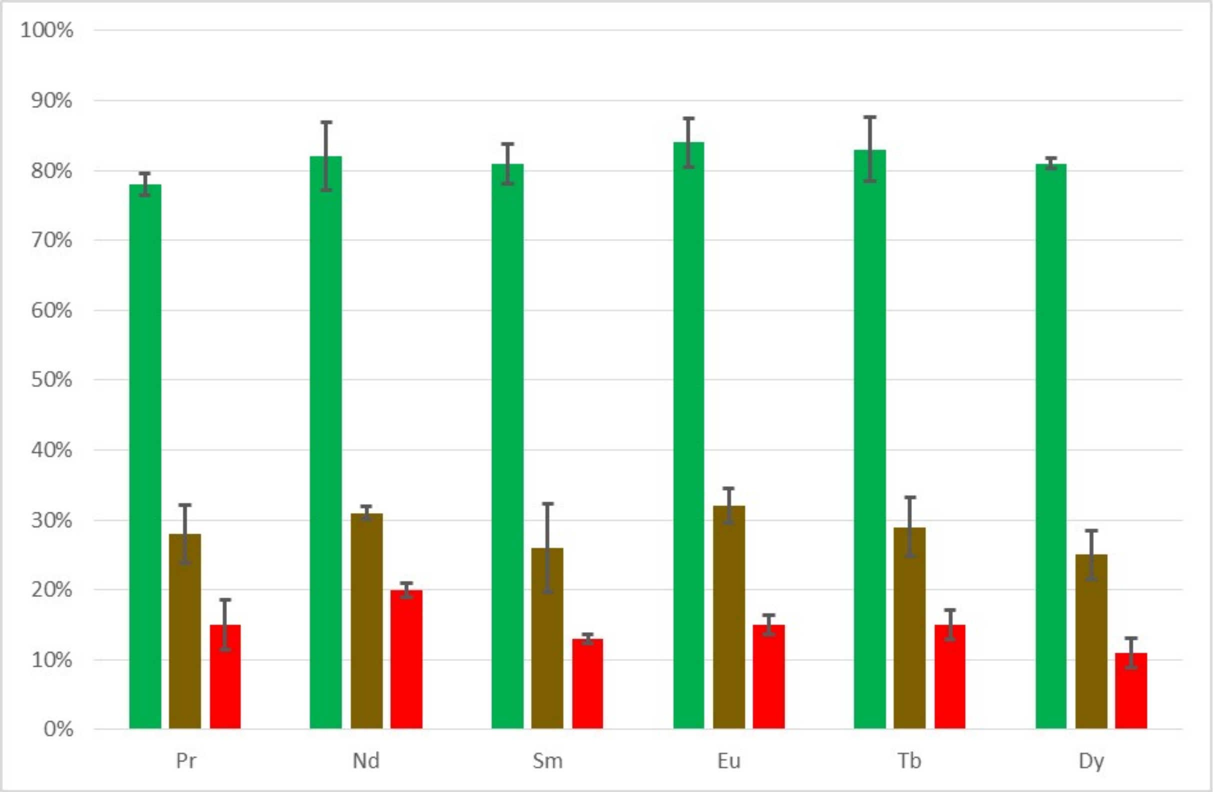

Figure S17: Capture efficiency E_S by CO_2-induced self-assembling of rare earth metals (green), diethylenetriamine (brown) and trifluoroacetate (red) from methanolic samples ($c_0 = 0.5$ M, $x_0 = 1/12$).

	n_S (mmol)				n_L (mmol)			L_S			E_S(%)			S(M/X)
M	$n_S(CO_2)$	n_S(DETA)	n_S(M)	n_S(X)	n_L(DETA)	n_L(M)	n_L(X)	L_S(CO2)	L_S(M)	L_S(X)	E_S(DETA)	E_S(M)	E_S(X)	
Pr	2.22	1.39	0.33	.18	3.65	0.09	1.05	1.60	0.23	0.13	28	78	15	21.4
Nd	2.53	1.57	0.34	0.24	3.43	0.07	0.95	1.61	0.22	0.15	31	82	20	19.2
Sm	2.08	1.32	0.31	0.16	3.79	0.07	1.01	1.58	0.24	0.12	26	81	13	28.0
Eu	2.54	1.65	0.35	0.25	3.44	0.06	0.95	1.54	0.21	0.15	32	84	20	22.2
Tb	2.14	1.33	0.34	0.17	3.27	0.07	1.01	1.61	0.25	0.13	29	83	15	28.9
Dy	1.97	1.19	0.30	0.12	3.62	0.07	1.03	1.66	0.25	0.10	25	81	11	36.8

Table S1: Compositional analyses of solid/liquid phases (in mmol) with varying metals ($n_0(M) = 0.416$ mmol; $n_0(DETA) = 5.0$ mmol; $n_0(X) = 1.25$ mmol)

	$P_S(M/CO_2)$				$P_S(CO_2/M)$				$x_3 = P_S(DETA/2.CO_2)$			
	max	min	moy	Δ	max	min	moy	Δ	max	min	moy	Δ
Pr	100%	82%	91%	18%	45%	36%	41%	8%	80%	60%	70%	20%
Nd	100%	76%	88%	24%	40%	31%	36%	9%	81%	61%	71%	20%
Sm	100%	83%	91%	17%	45%	37%	41%	8%	79%	58%	69%	21%
Eu	100%	76%	88%	24%	41%	31%	36%	10%	77%	54%	66%	23%
Tb	100%	83%	92%	17%	48%	40%	44%	8%	81%	61%	71%	20%
Dy	100%	87%	93%	13%	46%	40%	43%	6%	83%	66%	75%	17%

Table S2: Building block pairing and carbamate repartition for varying metals ($n_0(M) = 0.416$ mmol; $n_0(DETA) = 5.0$ mmol; $n_0(X) = 1.25$ mmol)

Details of the calculations:

$$\% \, P_s(i/j) = \frac{n_s(i/j)}{\sum_k n_s(i/k)}$$

Where $\% \, P_s(i/j)$ is the percentage of the building block *i* paired with the building block *j*.

$$\% \, P_s(M/X) = \frac{n_s(M/X)}{n_s(M/X) + n_s(M/CO_2)}$$

In extreme cases, either all trifluoroacetates are paired with metal or none are paired. Giving:

$$\% \, P_s(M/X)_{max} = \frac{n_s(X)}{3n_s(M)} \; et \; \% \, P_s(M/X)_{min} = 0$$

$$\% \, P_s(M/X)_{moy} = \frac{n_s(X)}{6n_s(M)}$$

Hence:

$$\% \, P_s(M/CO_2)_{min} = 1 - \frac{n_s(X)}{3n_s(M)} \; et \; \% \, P_s(M/CO_2)_{max} = 1$$

$$\% \, P_s(M/CO_2)_{moy} = 1 - \frac{n_s(X)}{6n_s(M)}$$

Similarly for carbamate – ammonium *vs.* metal-carbamato pairing:

$$\% \, P_s(CO_2/M) = \frac{n_s(CO_2/M)}{n_s(CO_2/M) + n_s(CO_2/RR'NH_2)}$$

$$\% \, P_s(CO_2/M)_{min} = \frac{3n_s(M) - n_s(X)}{n_s(CO_2)} \quad and$$

$$\% \, P_s(CO_2/M)_{max} = \frac{3n_s(M)}{n_s(CO_2)}$$

$$\% \, P_s(CO_2/M)_{moy} = \frac{6n_s(M) - n_s(X)}{2n_s(CO_2)}$$

Regarding the fraction of dicarbamates among the DETA – CO_2 adducts, by definition of the loading in CO_2 is:

$$L_S(CO_2) = \frac{n_2 + 2n_3}{n} = x_2 + 2x_3 = 1 + x_3 - x_1$$

The molar fraction x_3 of dicarbamates **3** with respect to either the molar fraction x_1 of free DETA **1** or x_2 of monocarbamate **2** can be easily be deduced:

$$x_3 = \frac{L_S(CO_2) - x_2}{2} \; or \; x_3 = L_S(CO_2) - 1 - x_1,$$

providing the maximal (no monocarbamate **2**), minimal (no free DETA **1**) and average values for x_3 respectively :

$$x_{3max} = \frac{L_S(CO_2)}{2} \, ; \, x_{3min} = L_S(CO_2) - 1$$

$$x_{3moy} = \frac{3L_S(CO_2) - 2}{4}$$

2.2.1.2. Influence of the initial metal/DETA stoichiometry x_0(M)

	n_S (mmol)				n_L (mmol)			L_S			E_S(%)			S(M/X)
X_0(M)	$n_S(CO_2)$	n_S(DETA)	n_S(M)	n_S(X)	n_L(DETA)	n_L(M)	n_L(X)	L_S(CO2)	L_S(M)	L_S(X)	E_S(DETA)	E_S(M)	E_S(X)	
1/24	0.983	0.650	0.143	0.040	4.359	0.065	0.573	1.51	0.22	0.06	13	69	6	31.5
1/12	2.324	1.543	0.353	0.220	3.412	0.071	1.036	1.51	0.23	0.14	31	83	12	39.5
1/6	1.69	1.13	0.37	0.24	1.33	0.02	0.89	1.50	0.35	0.21	46	95	22	68.6

1/3	2.37	1.29	0.78	0.31	0.90	0.05	1.07	1.83	0.60	0.24	59	94	23	53.8

Table S3: Compositional analyses of solid/liquid phases (in mmol) with varying initial Nd^{3+} /DETA stoichiometries x_0(M) (c_0(DETA) = 0.5 mol.L^{-1})

	$P_S(M/CO_2)$				$P_S(CO_2/M)$				$x_3 = P_S(DETA/2CO_2)$			
X0	max	min	moy	Δ	max	min	moy	Δ	x_{3max}	x_{3min}	x_{3moy}	Δx_3
1/24	100%	91%	95%	9%	44%	40%	42%	4%	76%	51%	63%	25%
1/12	100%	79%	90%	21%	46%	36%	41%	9%	76%	51%	63%	25%
1/6	100%	78%	89%	22%	66%	51%	59%	14%	75%	50%	63%	25%
1/3	100%	87%	93%	13%	99%	86%	92%	13%	92%	83%	87%	9%

Table S4: Building block pairing and carbamate repartition for varying initial Nd^{3+} /DETA stoichiometries x_0(M) (C_0(DETA) = 0.5 mol.L^{-1})

2.2.1.3. Influence of the initial concentration c_0(DETA)

	Ns				nL			LS			ES(%)			S(M/X)
c0	$n_S(CO_2)$	n_S(DETA)	n_S(M)	n_S(X)	n_L(DETA)	n_L(M)	n_L(X)	L_S(CO2)	L_S(M)	L_S(X)	E_S(DETA)	E_S(M)	E_S(X)	
0.05	1.30	0.73	0.40	0.01	4.17	0.02	1.34	1.79	0.54	0.02	15	96	1	2376
0.1	1.69	0.90	0.35	0.01	3.73	0.03	0.79	1.87	0.39	0.01	20	92	2	922
0.25	2.27	1.28	0.32	0.11	3.82	0.06	1.05	1.78	0.25	0.08	25	84	10	51
0.5	2.32	1.54	0.35	0.22	3.41	0.07	1.04	1.51	0.23	0.14	31	83	11	39
1	2.12	1.39	0.28	0.26	3.18	0.09	0.89	1.50	0.33	0.22	30	75	23	11
1.5	7.17	5.35	0.87	0.97	8.45	0.27	2.11	1.83	0.60	0.24	39	76	31	7

Table S5: Compositional analyses of solid/liquid phases (in mmol) with varying initial c_0(DETA) (x_0(M) = 1/12)

	$P_S(M/CO_2)$				$P_S(CO_2/M)$				$x_3 = P_S(DETA/2CO_2)$			
C_0	max	min	moy	Δ	max	min	moy	Δ	x_{3max}	x_{3min}	x_{3moy}	Δx_3
0.05	100%	99%	100%	1%	78%	78%	78%	1%	90%	79%	84%	11%

0.1	100%	99%	100%	1%	62%	62%	62%	1%	94%	87%	90%	6%
0.25	100%	89%	94%	11%	42%	37%	40%	5%	89%	78%	84%	11%
0.5	100%	79%	90%	21%	45%	36%	41%	9%	76%	51%	63%	25%
1	100%	69%	85%	31%	40%	27%	33%	12%	75%	50%	63%	25%
1.5	100%	63%	81%	37%	36%	23%	30%	14%	92%	83%	87%	9%

Table S6: Building block pairing and carbamate repartition for varying initial c_0(DETA) (x_0(M)= 1/12)

2.2.2. Bimetallic systems

		L_S				E_S(%)				$S(M_2/M_1)$
M_1/M_2	C_0	L_S(CO2)	$L_S(M_1)$	$L_S(M_2)$	L_S(X)	E_S(DETA)	$E_S(M_1)$	$E_S(M_2)$	E_S(X)	
Fe/Nd	0.5M	1.57	0.10	0.35	0.02	14	20	73	1	22
Fe/Nd	0.05M	1.48	0.08	0.26	0.03	25	34	90	0	32
Co/Sm	0.5M	1.30	0.05	0.13	0.13	14	19	79	7	17
Co/Sm	0.05M	1.37	0.02	0.10	0.10	6	2	0.71	1	106

Table S7: Compositional analyses of solid/liquid phases (in mmol) with varying initial c_0(DETA) and bimetallic system ($x_0(M_1+M_2)$ = 1/12)

		$P_S(M/CO_2)$				$P_S(CO_2/M)$				$x_3 = P_S(DETA/2CO_2)$			
M_1/M_2	C_0	max	min	moy	Δ	max	min	moy	Δ	x_{3max}	x_{3min}	x_{3moy}	Δx_3
Fe/Nd	0.5M	100%	99%	100%	1%	78%	78%	78%	1%	81%	61%	71%	20%
Fe/Nd	0.05M	100%	98%	99%	2%	91%	89%	90%	2%	76%	52%	64%	24%
Co/Sm	0.5M	100%	76%	88%	24%	42%	32%	37%	10%	76%	51%	63%	25%
Co/Sm	0.05	100%	72%	86%	28%	26%	19%	23%	7%	76%	51%	63%	25%

Table S8: Building block pairing and carbamate repartition for varying initial c_0(DETA) and bimetallic system ($x_0(M_1+M_2)$ = 1/12)

References

(1) C. Rüssel, *J. Non-Cryst. Solids*, 1993, **152**, 161-166

(2) N. Iranpoor and H. Adibi, *Bull. Chem. Soc. Jpn*., 2000, **73**, 675-680

(3) M. J. Baillie, D. H. Brown, K. C. Moss and D. W. A. Sharp, *J. Chem. Soc. A,* 1968, 3110-3114

(4) B. Vitorge, S. Bieri, M. Humam, P. Christen, K. Hostettmann, O. Muñoz, S. Loss and D. Jeannerat, *Chem. Commun.* 2009, 950.